112 年度行專訴第 11 號附圖

附圖一：

第 6 圖係系爭專利之發明之一光學濾波器之一剖面之一示意性圖解說明

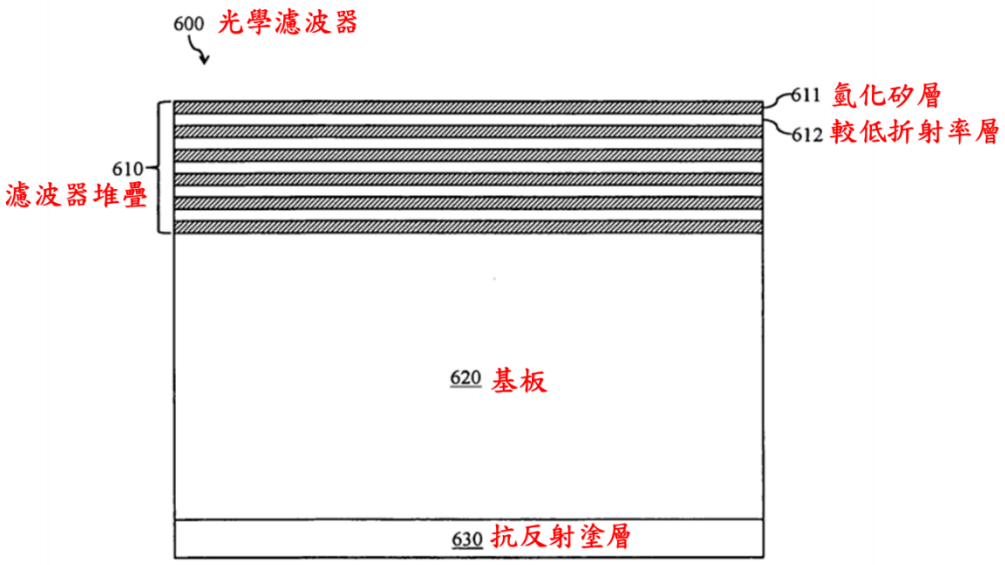


圖 6

圖 7A 係比較圖 1 之第一習用光學濾波器與根據本發明之一第一例示性光學濾波器之性質之一表

第一習用光學濾波器與第一例示性光學濾波器之比較		
性質	第一習用光學濾波器	第一例示性光學濾波器
半峰全幅值(nm)	66.0	46.5
中心波長移位，0°至30°(nm)	-29.1	-12.2
2856 K 黑體之背景透射率(%)	14.8	9.75
總塗層厚度(nm)	24432	5688

圖 7A

圖 7D 係係第一例示性光學濾波器在 0°及 30°之入射角下之透射光譜之一曲線圖

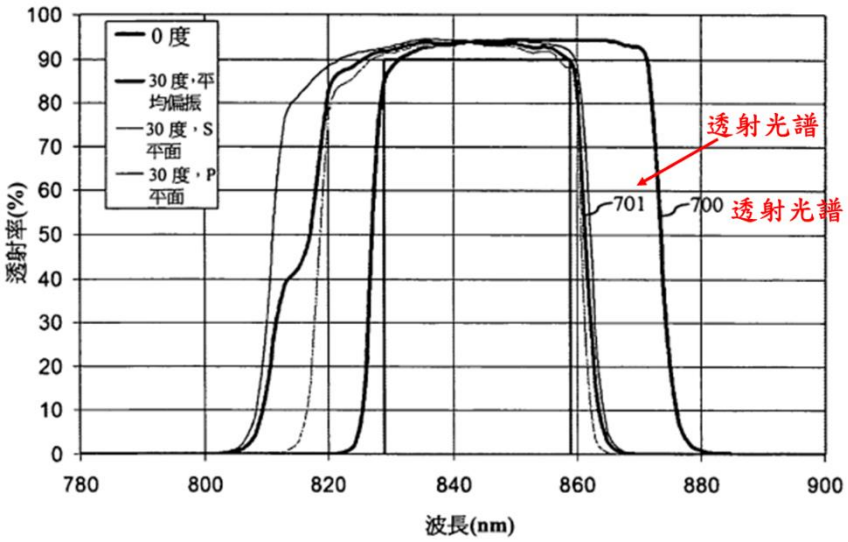


圖 7D

1 **附圖二:**

第 10 圖係帶通濾波器的結構的截面圖

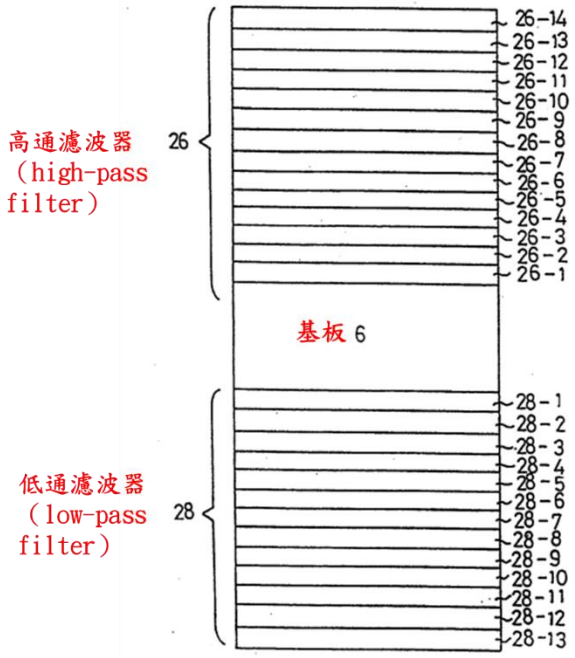


FIG.10

表 1 係圖 4 濾波器結構描述表

TABLE 1

Layer No.	Material	Geometrical thickness (nm)	Optical thickness (nm)	Refraction index (λ_o = 500 nm)
Substrate	Corning 7059 glass	200		1.52
26-1	a-Si:H	11.42	41.3	3.62-0.3i
26-2	a-SiNx:H	130.7	237.9	1.82
26-3	a-Si:H	33.47	121.2	3.62-0.3i
26-4	a-SiNx:H	77.06	140.2	1.82
26-5	a-Si:H	58.68	212.4	3.62-0.3i
26-6	a-SiNx:H	42.10	76.6	1.82
26-7	a-Si:H	85.26	308.6	3.62-0.3i
26-8	a-SiNx:H	52.50	95.6	1.82
26-9	a-Si:H	50.21	181.8	3.62-0.3i
26-10	a-SiNx:H	86.17	156.8	1.82
26-11	a-Si:H	48.49	175.5	3.62-0.3i
26-12	a-SiNx:H	66.85	121.7	1.82
26-13	a-Si:H	45.20	163.6	3.62-0.3i
26-14	a-SiNx:H	184.99	336.7	1.82
	Air			1

表 3 描述 13 層低通濾波器的結構參數

TABLE 3

Layer	Material	Geometrical thickness (nm)	Optical thickness (nm)	Refraction index (λ_o = 500 nm)
Substrate	Corning 7059 glass			1.52
28-1	a-SiNx:H	69.73	126.9	1.82
28-2	a-Si:H	99.84	361.4	3.62-0.3i
28-3	a-SiNx:H	177.52	323.1	1.82
28-4	a-Si:H	88.92	321.9	3.62-0.3i
28-5	a-SiNx:H	174.76	318.1	1.82
28-6	a-Si:H	87.56	317	3.62-0.3i
28-7	a-SiNx:H	173.24	315.3	1.82
28-8	a-Si:H	87.97	318.5	3.62-0.3i
28-9	a-SiNx:H	176.86	321.9	1.82
28-10	a-Si:H	87.21	315.7	3.62-0.3i
28-11	a-SiNx:H	174.12	316.9	1.82
28-12	a-Si:H	91.78	332.3	3.62-0.3i
28-13	a-SiNx:H	72.72	132.3	1.82
	Air			1

第 12 圖係帶通濾波器的透射率曲線

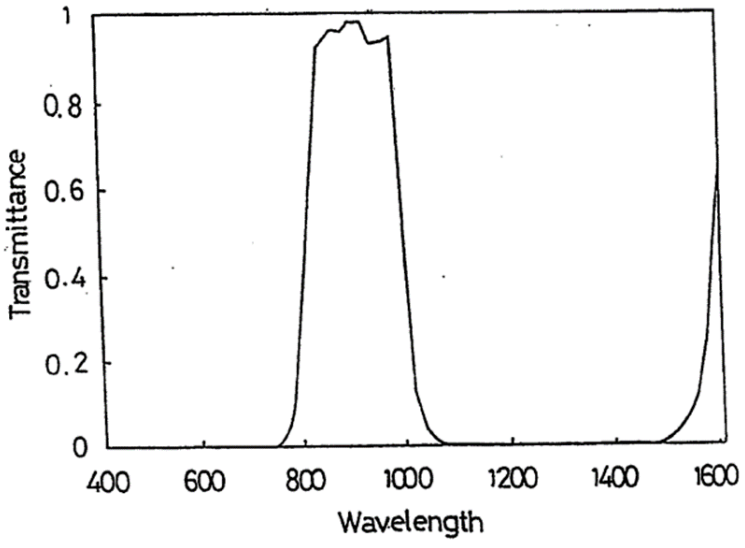


FIG.12

附圖三:

第 4 圖係α-Si:H 和 Si:H 的折射率和消光係數是波長的函數

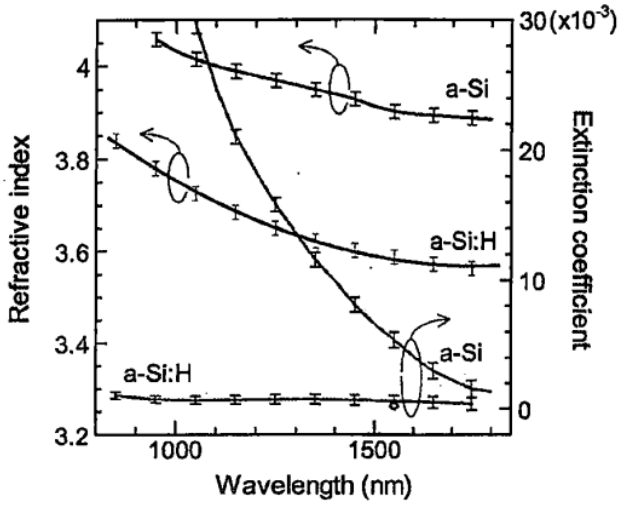


Fig. 4. Refractive index and extinction coefficient of α-Si:H and Si:H as functions of wavelength.

附圖四:

典型曲線顯示有效指數 n*如何隨順序編號變化在圖 7.11 內顯低折射率和高折射率墊片情況

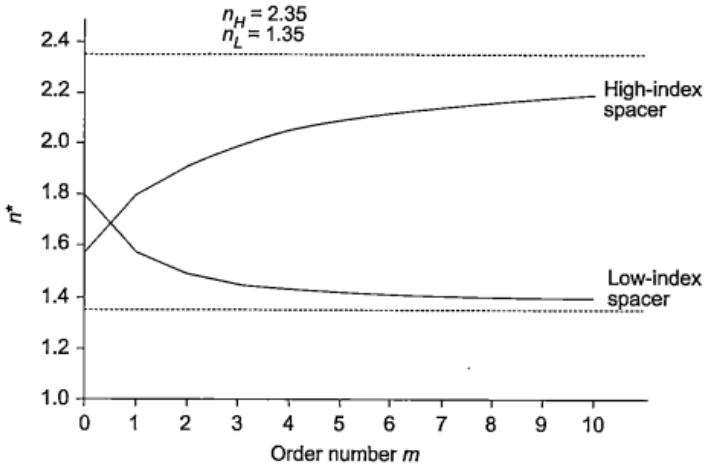


Figure 7.11. The effective index n^* plotted against order number m for Fabry–Perot filters constructed of materials such as zinc sulphide, $n = 2.35$, and cryolite, $n = 1.35$. The results were calculated from expressions (7.35) and (7.36).

附圖五:

圖 2 係非晶矽的折射率隨著氫濃度和總系統壓力的增加而降低

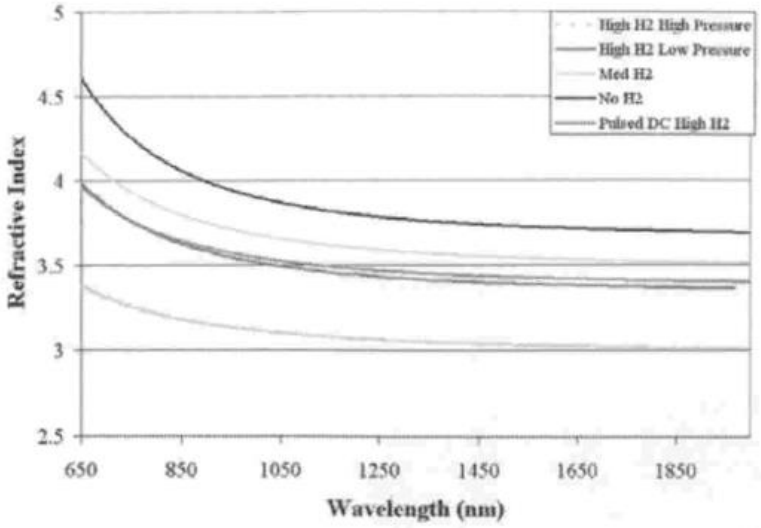


Figure 2: The refractive index of the a-Si shows a decrease in index as the hydrogen concentration and total system pressure increase. All samples were produced using the 40 kHz AC process, except where noted.

圖 3 係非晶矽的消光係數隨著氫氣濃度和總系統壓力的增加而降低

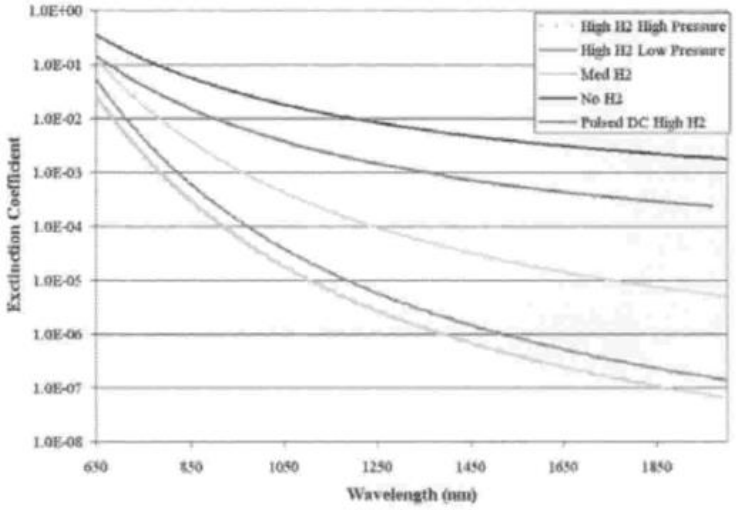


Figure 3: The extinction coefficient of the a-Si decreases as the hydrogen concentration and total system pressure increase. Note how much lower the extinction coefficient for the High H2. High Pressure AC process is compared with the same conditions for the pulsed DC Process.

附圖六:

圖 6 係示例性光伏裝置中示例性材料折射率的折射率（n）對波長（nm）之曲線圖

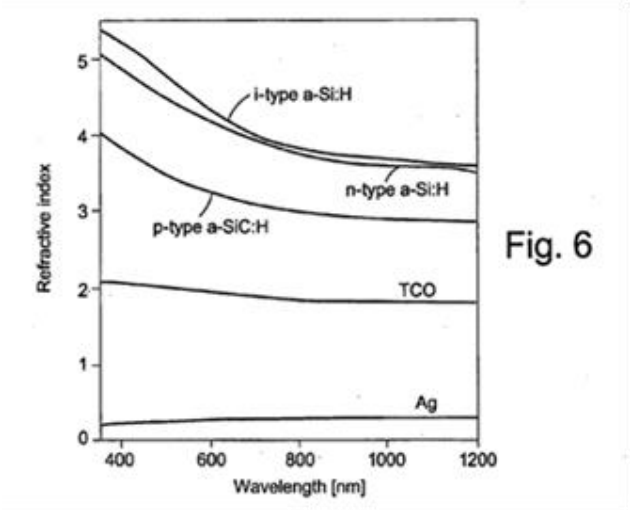


Fig. 6

附圖七:

表 2 係 a-Si:H 與 a-SiNx：H 薄膜的平均色散折射率

Table 2. Averaged Dispersive Refractive Indices of a-Si:H and a-SiN_x:H Thin Films

Wavelength (nm)	$n-ik$	
	(a-Si:H)	(a-SiN_x:H)
400	3.650–*i*0.500	1.830–*i*0.002
500	3.620–*i*0.300	1.820
600	3.600–*i*0.100	1.800
700	3.570–*i*0.040	1.790
800	3.530–*i*0.004	1.785
900	3.470	1.780
1000	3.400	1.776
1200	3.350	1.770
1500	3.340	1.765

圖 5(a)及(b)係五層帶通濾波器的實測光譜透射率曲線

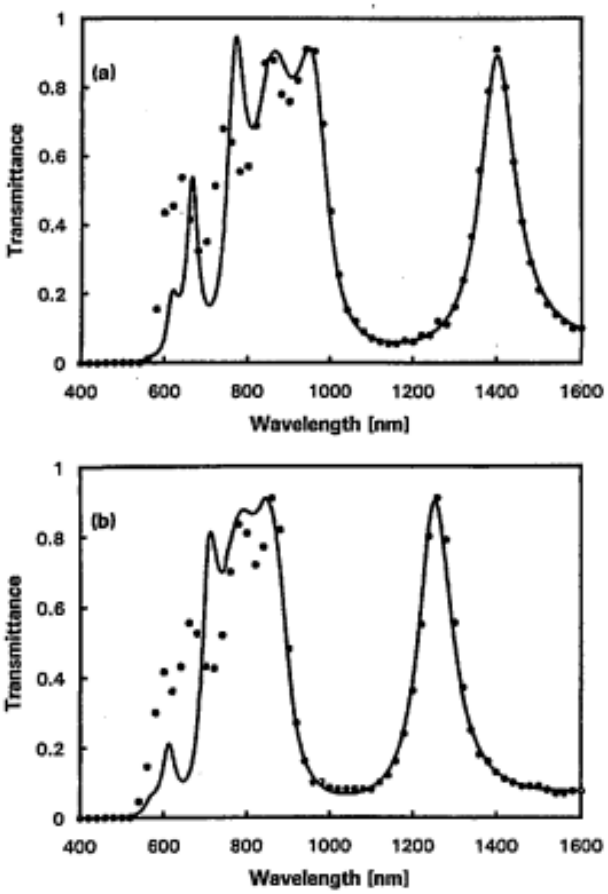


Fig. 5. Measured spectral transmittance curves of the five-layer bandpass filters. The solid curves and the filled circles represent the experimentally measured and the calculated spectral transmittances, respectively. (a) air/HLHHLH/glass, (b) air/0.96H0.96L0.96H0.96H0.96L0.96H/glass.